Desalination and Water Treatment
www.deswater.com

doi: 10.5004/dwt.2018.23148

135 (2018) 221–235
December

Synthesis of functionalized nanotube-C60 hybrid and its effect in the adsorption of Cu(II), Pb(II), Ni(II) from aqueous solutions

Najmeh Mehrmand[a], Mostafa Keshavarz Moravaji[a,b,*], Arsalan Parvareh[a,c]

[a]*Department Chemical Engineering, Borujerd Branch, Islamic Azad University, Borujerd, Iran*
email: naj451.mand@gmail.com (N. Mehrmand), moraveji@aut.ac.ir (M.K. Moravaji)

[b]*Department of Chemical Engineering, Amirkabir University of Technology (Tehran Polytechnic), Tehran, Iran*
email: a.parvareh@razi.ac.ir

[c]*Chemical Engineering and Petroleum Faculty, Razi University, Kermanshah, Iran*

Received 31 Mach 2018; Accepted 17 September 2018

ABSTRACT

In this work, the capability of hybrid of functionalized Carbon nanotube and fullerene (C60) as novel adsorbent was studied in order to remove copper, nickel and lead ions. This hybrid was tested for adsorption of heavy metals such as copper, nickel and lead, at pH 2 and 8 conditions for first time. At pH of 8 and for 30 min of the contact time, the concentration of lead, copper and nickel ions reached from 20 to 0.25, 5.4 and 18.07 ppm, respectively. For 30 min and pH 2, the percentage of removal of metal ions were about 13%. The results showed that the removal efficiency was low at pH 2 and high at pH 8. Also, after the metal ions adsorption, the recovery and regeneration process were done by placing adsorbent in strong acids for removing metals from their surface. The highest values of correlation coefficient (R^2) were obtained in the Pseudo-second-order model for adsorption of Pb (1), Cu (0.994) and Ni (0.981). The best adsorption isotherm models and correlation coefficients for each ion were Langmuir with 0.987 for Pb, Freundlich with 0.985 for Cu, and Freundlich with 0.999 for Ni.

Keywords: Functionalized carbon nanotube-C60 hybrid; Adsorption; Heavy metal; Optimal amount; Adsorption isotherm model

1. Introduction

Reducing water resources by enormous increase of water use, as well as the entry of various pollutants into water resources, has led to the global water crisis. The main reason of the current water crisis is pollution of water resources by chemical and biological contaminations, the increase of urbanization and its corresponding development of industries and agriculture. For many decades, the water crises have had a direct impact on the economic, social, environmental and political dimensions, which are the bases for the development of every country. Water pollutants can be divided into three categories: organic, inorganic and biological pollutants.

1. Organic pollutants: Organic compounds such as benzene, phenols [1], chlorine compounds [2], drugs [3], surfactants, etc., which easily enter the water cycle if a preventing approach is not implemented [4,5].
2. Mineral contaminants: Heavy metal contaminants, which are mostly due to industrial activities such as metalworking, chemical production, metallurgical industry, mining operations, soils around military bases and handicrafts can enter water resources [6,7].
3. Biological contaminants: Biological pollutants are divided into three groups: (a) microorganisms (bacteria, viruses, etc.) [8], (b) the presence of natural organic matter (NOM) [9,10], (c) bio-toxins [11].

Heavy metals are the metal elements with atomic number larger than 20 and atomic density larger than 4 g/cm^3 or 5 times larger than of the water [12]. Given this definition Hg, Pb, Ag, Cu, Cd, Cr, Zn, Ni, Co and Mn are identified as heavy metals and they are indeed the sources of water contamination. Some of these metals such as lead (Pb), nickel (Ni), cadmium (Cd), chromium (Cr), zinc (Zn)

*Corresponding author.

and mercury (Hg) are rare elements, and some of these metals, such as copper (Cu), selenium (Se) and zinc (Zn), are essential for maintenance of metabolism. These materials at higher concentrations can lead to poisoning.

There are several methods, mainly chemical and biological, for removing heavy metals from aqueous environments. In the last few decades, many studies have been carried out on broad range of nanomaterials to remove heavy metals from water. Carbon nanotubes and fullerenes have shown promising performance and are often used to adsorb a wide range of water pollutants [13–17].

The first fullerene molecule was discovered in 1985 by American chemist Robert Floyd Curl Jr, Richard Errett Smalley of Rice University in Houston, TX, and Sir Harold Walter Kroto of the University of Sussex in Brighton, England [18]. Carbon nanotubes were discovered by Iijimain [19].

Fullerenes and nanotubes are generally insoluble, and they become soluble by the addition of a suitable group that can covalently attached to them [20]. Numerous studies have been done on suitable functionalization of fullerenes and adjusting their properties. Fullerenes can be oxidized by using various oxidizing agents to create different number of OH, including dilute sulfuric acid and potassium nitrate (C60 $(OH)_{15}$) [21,22], sodium hydroxide diluted with tetra butyl ammonium hydroxide (TBAH) catalyst (60 $(OH)_{24–26}$) [23], sodium hydroxide [24] and hydrogen peroxide [25], by the hydrogen peroxide method (a multi-stage process with a mixture of peroxide and C60 (C60 $(OH)_8$)). The maximum number of hydroxyl groups that can be connected to C60 are about 36–40 [26]. In order to modify the surface of raw carbon nanotubes, the side walls can be functionalized by different groups [27,28]. Oxidation in acids can create functional groups containing oxygen, such as –OH and –COOH on the surface of the nanotubes [29,30].

Functionalizing the single-wall CNT with agents such as hydroxyl, carboxylic and carbonyl have been reported as a way to make CNT solvable in water with great sustainability [31,32]. With several strategies for combining these two allotropes, a variety of carbon nanotube-fullerenes hybrids are obtained [33]. The carbon nanotube–C60 hybrid was first discovered by Luzzi in 1998. They observed that several fullerenes connected to nanotubes were recovered as side products in the synthesis of single-wall carbon nanotubes [34]. Based on studies by Bourlinos et al. [35], a hybrid of nanotubes and C60s was synthesized. So far, this material has not been used to remove heavy metals. Using the method of Borelinos and colleagues, a hybrid is made of fullerols, sodium salt ($C60(OH)_{30}·25Na·30H_2O$) and nanotubes oxidized with nitric oxide [36–44].

The goal of current research is to evaluate hybrid of functionalized Carbon nanotube and fullerene (C60) as novel adsorbent in order to remove copper, nickel and lead ions. This hybrid is synthesized from CNTs and C60. The impact of different significant parameters such as pH, time (min), adsorbent amount (g) and initial ions concentration (mg/L) was experimentally. Two isotherm models involving Langmuir and Freundlich were used to fit the experimental data.

2. Materials

Materials for synthesis of hybrid are manufactured by the company EMFUTURE in Spain with the following specifications:

2.1. Carboxyl multiwall – CNT (MWCNT–COOH)

Characteristics: outer diameter 20–30 nm, inner diameter 5–10 nm, ash: <1.5 wt%, purity: >95 wt%, length 10–30 μm, special surface 110 m^2/g, electrical conductivity >100 Siemens/cm, bulk density 0.28 g/cm^3, actual density ~2.1 g/cm^3, and multiwall nanotubes contain 1.2% carboxylic group.

2.2. C60

Carbon fullerenes C60 appearance: granular powder, dark brown. When sublimed appears as deep blue-black needle-like crystals reaching 5 mm. Thin C60 films (<5 microns) appear golden-brown and it is insoluble in water. Characteristics: outer diameter ~ 1 nm, purity 99.5, molar mass 720.66 $g·mol^{-1}$, appearance: dark needle-like crystals, density: 1.65 g/cm^3.

3. Synthesis method

Based on the method of Bourlinos and colleagues, [35] the nanotube –C60 hybrid was synthesised (Fig. 1). Implementing this method with some changes, the CNT–

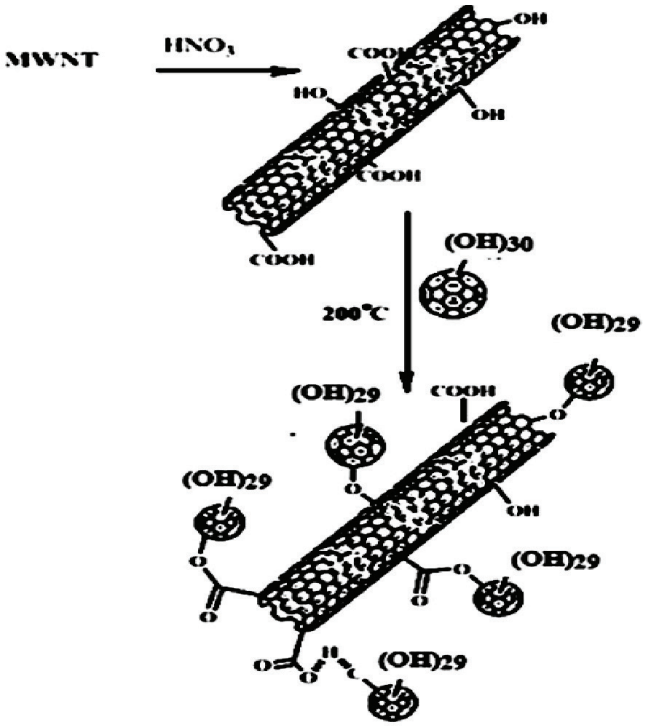

Fig. 1. Synthesis of CNT–C60 hybrid-based on the method of Bourlinos [35].

C60 hybrid was synthesized and tested in the labs of Sharif University of Technology. Then measurements of the heavy metals adsorption were carried out on in these labs. In this research, instead of fullerol sodium salt, the oxidized C60 is used for synthesis of the hybrid.

3.1. C60 oxidation

3 g of pure C60 were added to 750 ml of concentrated nitric acid (67%). The mixture was suspended by sonication for 10 min in order to more disperse C60. Then the temperature of mixture was slowly raised up to 115°C, and the mixture was refluxed for 6 h. After cooling materials at ambient temperature, the mixture was washed with the de-ionized water several times until solution pH reached to 7. In order to completely dry the solids, they were heated up to 80°C. The final products are dark brown solids (oxidized C60), which are soluble in water.

3.2. Synthesis of nanotube-C60 hybrid

Three grams of oxidized C60 were suspended in 300 ml de-ionized water and sonicated for 10 min in order to disperse them more. 9 g of carboxylic nanotube were suspended in the mixture and sonicated for 10 min (the amount of oxidized C60 to carboxylic nanotube is 1:3 weights). The mixture was refluxed for 6 h and then was heated at 80°C for 8 h in order to completely evaporate the remained water. The residue solids were heated at 200°C for 24 h and then were washed with the de-ionized water several times until solution pH reached to 7. This procedure is carried out to remove the soluble particles in the previous steps. Finally, the solids were dried at 80°C and then used as hybrids in the absorption experiments.

4. Experimental methods

In order to study the adsorption process, three compounds of lead, copper and nickel nitrate were selected. According to the studies carried out on nanotubes, most of the time, lead and nickel have the highest and lowest adsorption rates on the nanotubes, respectively.

Adsorption rate of copper metal falls between those of lead and nickel. This is the reason that these three metals have been chosen to demonstrate better absorption performance of the hybrid. To better analyze the results of metal adsorption on the hybrid, it is necessary to pay more attention to the chemical reaction of these metal solutions in the acidic and alkaline environments and their solubility in the temperature range 20–30°C in Tables 1 and 2.

For better investigation of waters contaminated with heavy metals, three metals with equal concentrations were selected as a multiple-metals adsorption. The ICP experiments were carried out in two pH 2 and 8, at temperature 25°C and contact time from 0 to 180 min with 30 min intervals. The amount of adsorbent and the concentration of each metal are 0.1 g and 20 ppm, respectively. The experiments were performed as batches. The adsorption process in acidic pH condition was evaluated by changing dose of the adsorbents. To adjust the pH of the acidic and alkaline, the nitric acid (1 mol/l.65%) and Na_2CO_3 (1 mol/l) were used, respectively.

Before carrying out experiments, the initial amount of the three metal elements in the hybrid were measured. The results of the elemental decomposition analysis of the hybrid have been shown in Table 3. The results showed that the amount of nickel in the hybrid was so high that it can strongly affected the adsorption of heavy metals, especially

Table 1
Equations for the reaction of heavy metals in acidic and alkaline environments

Metal's nitrate	PH	Equations reaction
Nickel	Base	$Ni(NO_3)_{2(aq)} + Na_2CO_{3(aq)} \rightarrow NiCO_{3(s)} + 2NaNO_{3(aq)}$
		$Ni(NO_3)_2 + HNO_3 \rightarrow Ni(NO_3)_2 + NO_2 + H_2O$
	Acid	$3NO_2 + H_2O \rightarrow 2H^+ + 2NO_3^- + NO$
Copper	Base	$Cu(NO_3)_{2\,(aq)} + Na_2CO_{3\,(aq)} \rightarrow CuCO_{3(s)} + 2NaNO_{3(aq)}$
	Acid	$Cu(NO_3)_2 + HNO_3 \rightarrow Cu(NO_3)_2 + NO_2 + H_2O$
Lead	Base	$Pb(NO_3)_{2(aq)} + Na_2CO_{3(aq)} \rightarrow 2NaNO_{3(aq)} + PbCO_{3(s)}$
		$HNO_3 + Pb(NO_3)_2 \rightarrow HNO_3 + Pb(NO_3)_2$
	Acid	$2H_2O + Pb(NO_3)_2 \rightarrow 2HNO_3 + Pb(OH)_{2(s)}$

Table 2
Solubility of metals compounds solutions in water

Solubility in water (g/100 ml Water) [45]			
Substance	Formula	20°C	30°C
Nickel(II) nitrate	$Ni(NO_3)_2$	94.2	105
Sodium carbonate	Na_2CO_3	21.5	39.7
Nickel(II) carbonate	$NiCO_3$	9.643×10^{-4}	–
Copper(II) nitrate	$Cu(NO_3)_2$	125	156
Copper(II) carbonate	$CuCO_3$	1.462×10^{-4}	–
Sodium nitrate	$NaNO_3$	87.6	94.9
Lead(II) hydroxide	$Pb(OH)_2$	1.615×10^{-4}	–
Lead(II) carbonate	$PbCO_3$	7.269×10^{-5}	–
Lead(II) nitrate	$Pb(NO_3)_2$	54.3	63.4

Table 3
Initial amounts of heavy metal in the hybrid adsorbents

The amounts of heavy metal in the adsorbents (ppm)			
Sample	Cu	Ni	Pb
CNT–C60 hybrid	13	342	<0.1
CNT–C60 hybrid (acid-treatment)	7	68.9	<0.01

nickel. For removal of nickel and impurities from hybrid surface, which are generated in the production stage, the hybrid was placed in the strong acid nitric for few hours and then was washed with de-ionized water several times until solution pH reaches to 7. Finally, the hybrid was dried for adsorption tests.

5. Results

5.1. SEM analyses

The morphologies of nanomaterials were measured with FE-SEM (Tescan Mira 3 LMU). In Fig. 2a, the outer diameters (ODs) measured before adsorption for the hybrid were 33.23–43.25. In Fig. 2a the measured ODs after adsorption were 34.97–45.20 nm. The OD for the carboxyl nanotube and C60 was 20–30 nm and 1 nm, respectively. The minimum diameter before and after sorption of the hybrid was greater than the maximum total diameter of carboxylic nanotube and C60, which indicated before sorption, the oxidized C60 agents were placed on the surface of carboxylic nanotubes. Also after sorption, oxidized metals were located on the surface of hybrids.

5.2. XRD analysis

The XRD diagrams of CNT–COOH, C60 $(OH)_n$, hybrid, and comparison between CNT–COOH and hybrid have been shown in Figs. 3a–d. These diagrams indicated that there were C60(OH)n compound in the hybrid. According to Table 4, the highest peaks in of the CNTs–COOH and hybrids were shown in the 2θ = 25.83,6.83, 12.41, 18.38, 14.3 8 and 2θ = 25.76, 20.90, 10.94, 17.87, 8.50, respectively. It is clear the nanotubes have been covered with oxidized C60 which are clearly observed in Fig. 3d.

Table 4
The highest values of XRD peaks for different samples

Samples	CNT–C60 hybrid		C60 oxide		CNT–COOH	
Decrease peak	2θ°	lob (cts)	2θ°	lob (cts)	2θ°	lob (cts)
	25.76	6765.41	10.94	94368.85	25.85	3230.00
	20.90	5862.37	31.01	93761.00	6.83	2728.80
	10.94	5078.08	20.90	89239.60	12.41	2327.91
	17.87	4728.12	17.81	22352.00	18.38	2163.90
	8.50	3084.83	28.21	8863.57	14.38	2140.29

5.3. FTIR analysis

The FTIR spectra of the hybrid were recorded in the range of 4000–400 cm^{-1}. The existence of the types of functional groups are confirmed by two diagrams of hybrid before and after adsorption that have been shown in Fig. 4. The peak located at 1,735.916 cm^{-1} with change percentage transmittance of 2.064 to 5.078 was due to stretching of carbonyl group. The peaks at 1,624.046, 1,450.45 and 1,201.64–1,274.93 cm^{-1} were related to the stretching vibration of the carboxyl (–C=O), carboxylic (–COO–) and C–O groups, respectively. The peaks at 3439.042 and 3234.59 cm^{-1} were related to the stretching vibration of the $C60(C(COOH)_2)_2$ and C60 $(OH)_n$, respectively. Fig. 4b shows the FTIR spectrum of Pb,Cu and Ni(II)-adsorbed on the hybrid. Due to the interaction of the functional groups on the hybrid with metal ions, the percentage transmittance and IR peaks shift to higher values. Shifting to lower and higher frequencies are indication off or motion of weaker and stronger bonds, respectively [46].

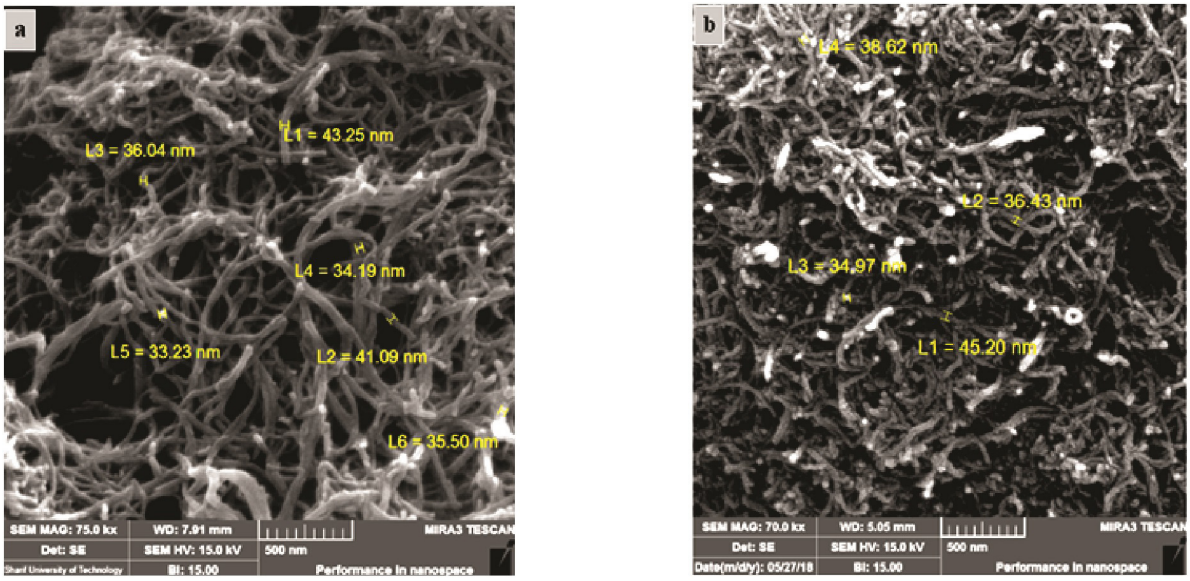

Fig. 2. FE-SEM morphology of: a) hybrid before adsorption, OD hybrid = 33.23–43.25 nm b) hybrid after adsorption OD hybrid = 34.97–45.20 nm.

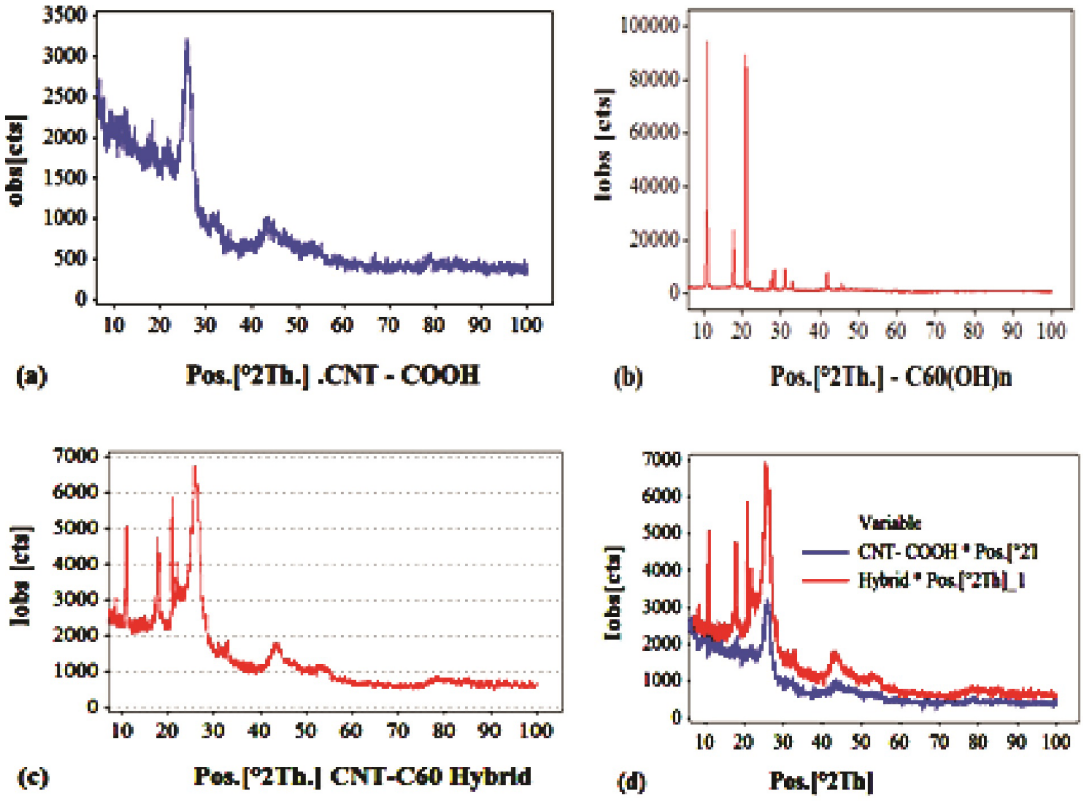

Fig. 3. XRD patterns of (a) CNT–COOH, (b) C60(OH)n, (c) hybrid, and (d) CNT–COOH and hybrid.

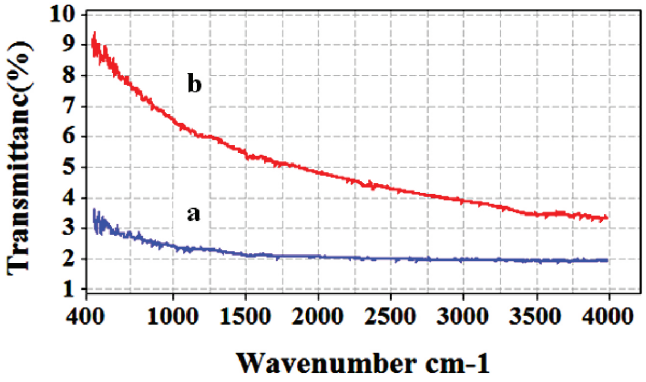

Fig. 4. FTIR spectra of (a) hybrid before adsorption, (b) after adsorption of metal ions.

The bands in the region 400–800 cm^{-1} are assigned to stretching vibrations of the meta-oxygen. The percentage transmittance is changed from 3.288–8.883 at band 499.409 cm^{-1} and 2.641–7.268 at 800.45 cm^{-1} that are corresponds asymmetric stretching vibration of metal oxide linkage.

5.4. BET analysis

The analysis data of the BET surface area of hybrid suggested that the surface area, size and total volume of pore can be changed before and after adsorption. The parameters are shown in Table 5. By looking at Table 5 one can see that surface area of hybrid is large. The BET surface area (m^2/g), pore size (nm), and diameter (<85.3896, 102.2139 nm) for range of pore volume (cm^3/g) of the hybrid before adsorption are 1625.93, 15.9, (6.46,7.40), and after adsorption reach to 1592.67,17.20, (6.86,7.82), respectively. It is shown in Figs. 5a,b that the main peak is centered at 82.10535 and 63.64649 nm before and after of adsorption, respectively. The N_2 adsorption/desorption isotherm of the

Table 5
Results of BET surface area analysis of hybrid before and after adsorption

Parameter of pores	Type of adsorption	Before adsorption	After adsorption
Surface area (m^2/g)	BET*	1625.93	1592.67
	Langmuir	2190.62	2149.03
	BJH	1860.75	1342.91
Total pore volume (cm^3/g)	Diameter < 85.3896 nm	6.46	6.86
	Diameter < 102.2139 nm	7.40	7.82
Adsorption average width(nm)	Adsorption BET	15.9	17.2
	Adsorption BJH	15.8	22.1

* Abbreviation: BET, Vrunauer-Emmett-Teller.

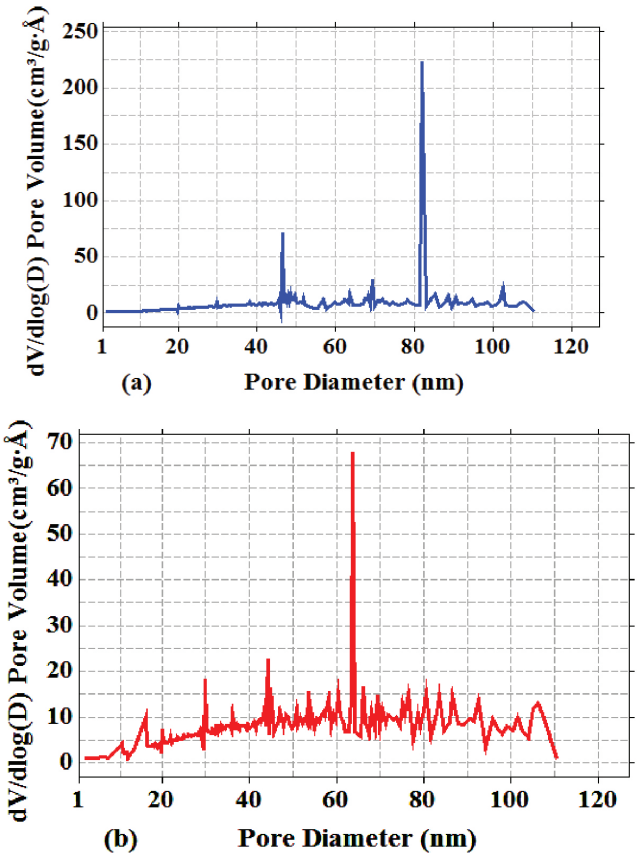

Fig. 5. Pore size distribution plots of the hybrid, (a) before adsorption, (b)after adsorption.

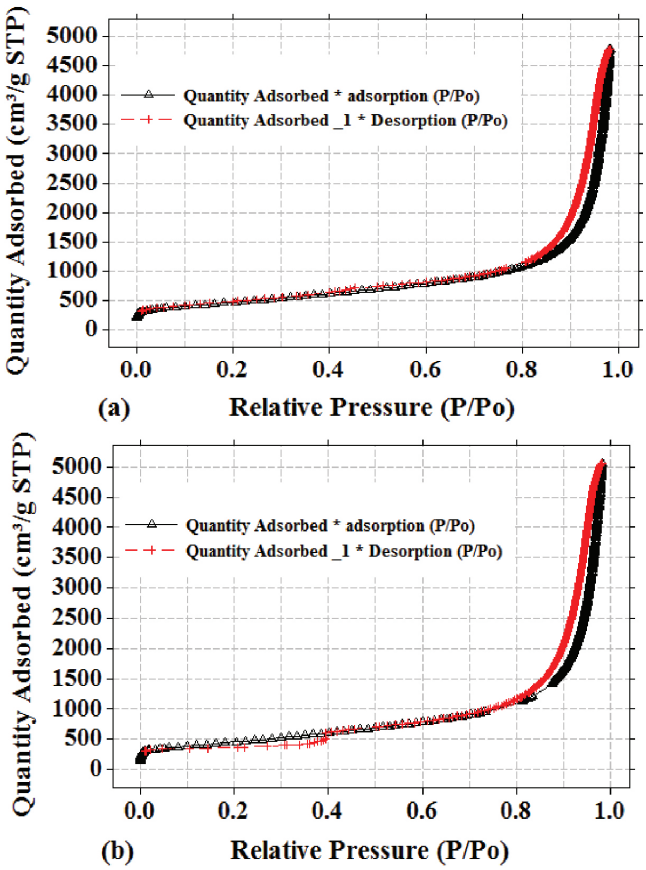

Fig. 6. Nitrogen adsorption-desorption isotherm plots of the hybrid, a) before adsorption and b) after adsorption.

hybrid before and after of adsorption shown in Figs. 6a, b. The isotherm is classified as type II. The hysteresis loop is type II and appears in the range 0.71.0 P/P°.

5.5. Effect of pH

5.5.1. Investigation of adsorption in alkaline environments

Lead: In absence of adsorbent, the concentration of lead ions is reduced from 20 to 3.93 ppm and the ions precipitate in the form of carbonate. In the presence of adsorbent for period of 30 min, the concentration reaches from 3.93 to 0.25 ppm.

Nickel: The concentration of nickel in the absence of adsorbent increases from 20 to 23.6 ppm. In alkaline environment, the concentration of nickel increases, due to the high solubility of nitrate nickel and the competition between metal ions in the solution. In the presence of adsorbent for 30 min, the concentration of nickel ions reached to 18.07 ppm, which indicates amount of nickel ions is reduced by 5.53 ppm.

Copper: The concentration of copper in solution is decreased from 20–17 ppm. This means that in the absence of adsorbent, 3 ppm of copper precipitate in the form of copper carbonate. After addition of hybrid for 30 min, the concentration of copper reaches from 17 to 5.4 ppm, almost 11.6 ppm are decreased of the concentration of copper metal (Fig. 7). At pH 8, before addition of the adsorbent, metals are deposited and their concentrations are gradually decreased in the solution.

At pH 8, some of the acidity solutions are used to neutralize the effect of alkaline of the sodium carbonate.

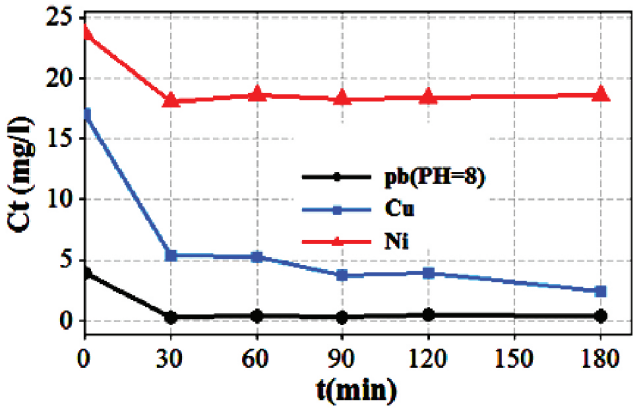

Fig. 7. Changes in concentrations of heavy metals in solution with time in alkaline environment (T = 25°C, W_{Hybrid} = 0.1 g, Ci_{Meial} = 20 mg/l, pH = 8).

The neutralization results in the formation of deposits and reduction of metal ions. Solubility of the copper, nickel and lead carbonates in alkaline environment are 1.462 × 10^{-4}, 9.643 × 10^{-4} and 7.269 × 10^{-5} (g/100 ml of water), respectively. A number of metal ions come out of solution in the form of precipitate. Therefore, all the sites on the hybrid surface could not be saturated. The maximum adsorption capacities for lead, copper and nickel are measured 9.88, 8.8, 0.965 mg/g, respectively.

5.5.2. Examination of adsorption in an acidic environment

Lead: Lead concentrations are constant in the absence and presence of adsorbent. With the addition of lead nitrate to water, lead hydroxide and nitric acid are produced. By increasing the amount of acid, the back reaction occurs that results in the production more lead nitrate. These are results of more the solubility and acidity (lower pH).

Nickel: The concentration of nickel reaches to 20 ppm in the absence of adsorbent. In the presence of adsorbent, the nickel concentration can become higher than 20 ppm, due to the high solubility of nickel nitrate and release of the nickel ions from the adsorbent surface.

Copper: The concentrations of copper in the absence and presence of adsorbent are 20 and 19.37 ppm, respectively. This difference is small. The high solubility of copper nitrate indicates the less adsorption. The results of adsorption experiments indicated that the concentration of metals in the environments with high acidity remains almost constant even when adsorbents are added to the solutions (Fig. 8). At this pH, the maximum adsorption capacities measured for lead, copper and nickel are 1.2, 1.23. 0.92 mg/g, respectively. The solubility of copper, nickel and lead nitrates are 125, 94.2 and 54.3 (g/100 ml of water), respectively.

At very low pH, the plenty of H^+ ions are generated in the solution and H^+ ions strongly compete with metal ions for the adsorption positions, and sites of adsorption on surface are very much saturated of H^+ ions. Therefore, small number of adsorption sites left for metal ions, which this in turn results in reduced adsorption of metals on the hybrid surface. It is believed that this property of low pH conditions can be further studied for removal of impurities and heavy metals from hybrid surface before and after adsorption. This means that for the recovery and regeneration of hybrids after adsorption, the hybrid should be placed at very acidic pH condition.

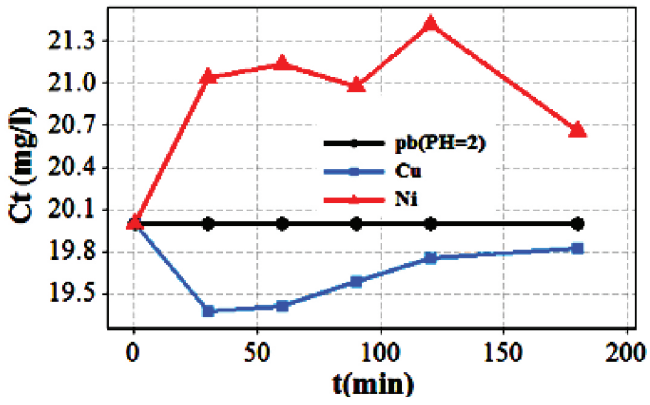

Fig. 8. Changes in concentration of heavy metals in solution with time, (T = 25°C, W_{Hybrid} = 0.1 g, Ci_{Metal} = 20 mg/l, pH = 2).

5.6. Effect of adsorbent dose

To determine the appropriate absorbent dose due to the higher sensitivity in absorption and reduction in the metal removal efficiency, the acidic environment is selected. The highest percentage of removal of metals is obtained at 0.06 g of adsorbent and for 30 min of contact time. At this dose, about 13% and 19% of the metals are removed from the solution before and after acid-treatment of hybrid. Although the contact surface increases with the increase of the adsorbent dose in the acidic environment, the percentage of removal of metals is greatly reduced as the repulsion is enhanced for adsorption on the hybrid surface. By looking at Fig. 9 one can see that the optimum adsorption occurs at the absorbent does of 0.06 g.

5.7. Effect of contact time

By increasing the contact time, the adsorption of metal on the adsorbent surface increases and reaches to a maximum value. The adsorption decreases by further increase of the contact time and eventually reaches to very small values. This different behavior is because the

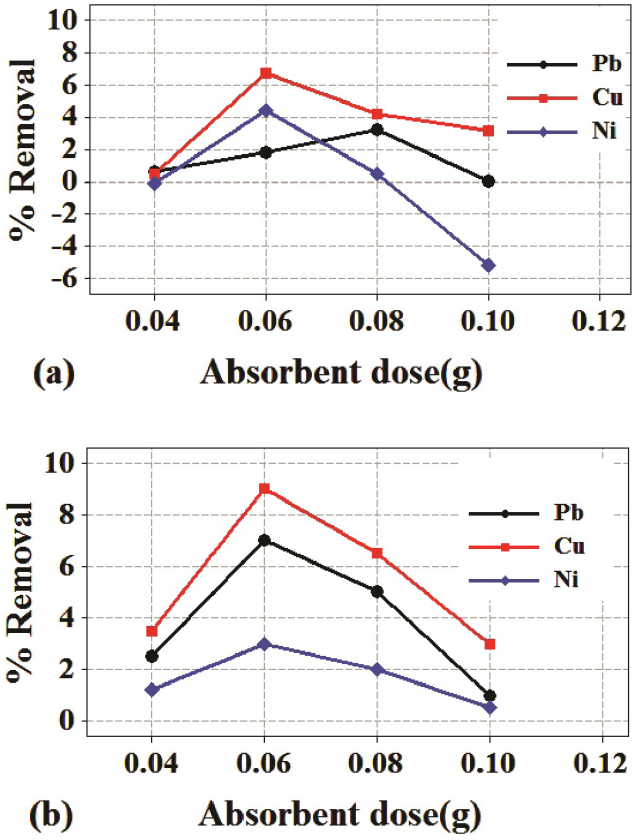

Fig. 9. Changes of the removal percentage with adsorbent dose, (a) before acid-treatement hybrid, (b) after acid-treatement hybrid. (T = 25°C, Ci_{metal} = 20 mg/l, t = 30 min, pH = 2).

adsorbent surface is completely covered by metals and other ions for a specific contact time period and there would not be surface adsorption cite available as the time goes on. In the acidic environment and for the contact time of 30 min the highest removal percentage for lead, copper and nickel are recorded at 0.08, 0.06, 0.06 g of adsorbent (Fig. 10).

The adsorption of copper and nickel ions are enhanced with the increase of contact time at 0–60 min, but more sharp increase of contact time was observed for each of three metal at 0–30 min. Therefore, the optimum of contact time can be selected 30 min.

5.8. Effect of initial concentration of heavy metals

The percentage of metal removal decreases with increasing the initial concentration of the metal within the medium. At the initial concentration of 10–50 mg/l, the removal percentages for lead, copper and nickel reaches to 90.5, 87.9 and 96.2, respectively. For smaller value of initial concentration, the removal percentages for lead, copper and nickel were 99.4, 99.8 and 99.52, respectively. In Fig. 11, it is observed that the optimal amount of initial concentrations is 20 mg/l, which after this concentration, the removal percentage decrease rapidly.

It is observed that the percentage removal strongly depends on the initial concentration of metals. At low initial concentrations, there are fewer metal ions that are ready to be absorbed on a certain number of unsaturated sites of hybrid. At higher concentrations, number of metal ions becomes more than the available adsorption cites, thus there would be more free metal ions that are freely remained in the solution. Thus by further increasing of the initial concentration the percentage of metal removal is decreased.

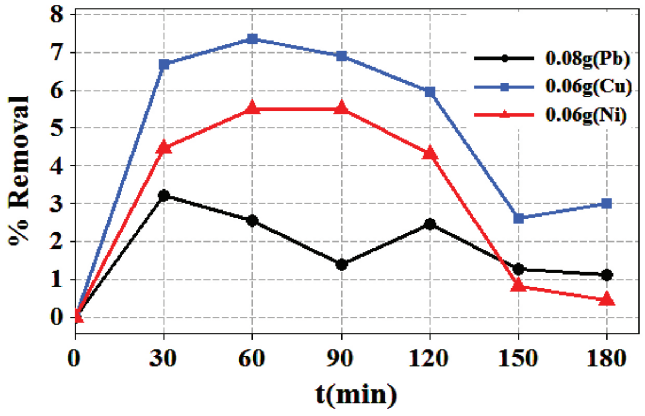

Fig. 10. Changes the percentage removal of heavy metals with time in various adsorbent doses, (T = 25°C, Ci_{Metal} = 20 mg/l, pH = 2).

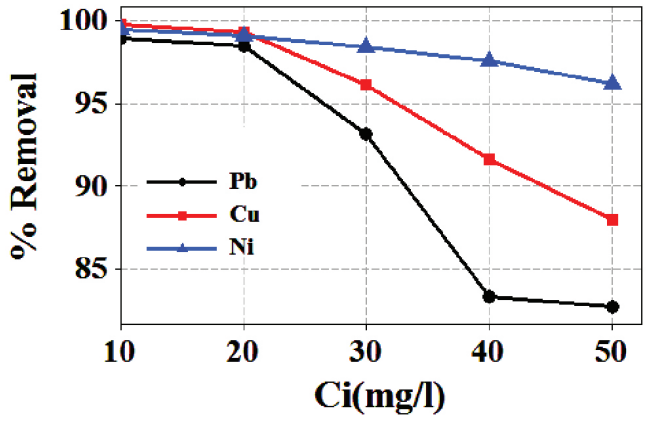

Fig. 11. Change in percentage of metal removal with initial concentration, (T = 25°C, PH = 8, t = 30 min, w_{Hybrid} = 0.06g).

5.9. Kinetics adsorption models

In this research, in order to study kinetics models for metals desorption onto hybrid surface we used pseudo-first-order, pseudo-second-order, intraparticle diffusion and Richie models. The equations of the kinetic models are given as in Eqs. (1–4):

5.9.1. Pseudo-first-order [47]

$$\text{In}\,(q_e - q_t) = \text{In}\,q_e - k_1 t \tag{1}$$

where q_e is the adsorption capacity at equilibrium (mg/g), q_t is the adsorption capacity at time t and k_1(min^{-1}) is the diffusion constant k_1 (Fig. 12a).

5.9.2. Pseudo-second-order [48]

$$\frac{t}{q_t} = \frac{1}{\left(k_2 \times q_e^2\right)} + \left(\frac{1}{q_e}\right)t \tag{2}$$

where q_e is the adsorption capacity at equilibrium (mg/g), q_t is the adsorption capacity at time t and k_2 is the diffusion constant (g mg^{-1}min^{-1}) (Fig. 12b).

5.9.3. Intra-particle diffusion [49]

$$q_t = k_{id}\sqrt{t} + C \tag{3}$$

where q_t is the adsorption capacity at time t, K_{id} is the intra-particle diffusion constant (mg/g min$^{0.5}$) and c (mg/g) is a constant that is related to the thickness of the boundary layer (Fig. 12c).

5.9.4. Richie [50]

$$\frac{1}{q_t} = \frac{1}{\left(k_R q_e t\right)} + \left(\frac{1}{q_e}\right) \tag{4}$$

where q_e is the adsorption capacity at equilibrium (mg/g), q_t is the adsorption capacity at time t and k_R is the rate constant (min^{-1}) (Fig. 12d).

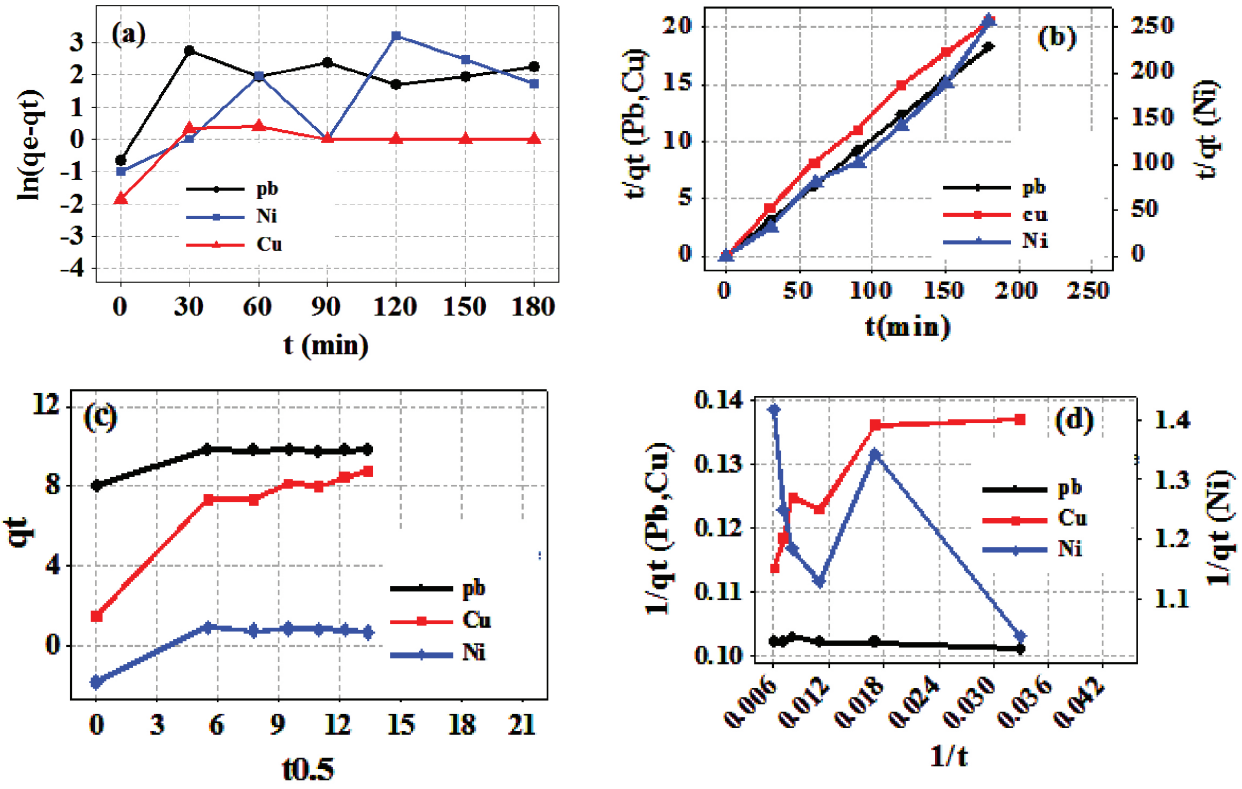

Fig. 12. kinetic models for adsorption (a) pseudo-first-order, (b) pseudo-second-order, (c) intra-particle diffusion (d) Richie model.

The plots of $ln(q_e - q_t)$, t/q_t, q_t and $1/q_t$ versus t, t , $t^{0.5}$ and $1/t$ respectively, should give a linear relationship, which the values of the adsorption parameters(k_1, q_e), (q_e, k_2), (C, k_{id}) and (q_e, k_R) can be determined for Eqs. (1)–(4) and the slope and intercept of the plots, respectively (Table 6).

The $q_{e,exp}$ and the $q_{e,cal}$ values from the pseudo-second-order and Richie kinetic models are very close to each other. The calculated correlation coefficients in the pseudo-second-order kinetic model are unit for lead and close to unit for copper and nickel, 0.994 and 0.981, respectively.

The transport of the metal ions from solution to the surface of the adsorbent may occur in one or several steps, such as: film, pore diffusion, surface diffusion and adsorption on the pore surface, or a combination of more than one step. The larger value of C in Eq. (3) denotes greater effects of the boundary layer. If graph of the q_t versus t demonstrates a linear relationship with the experimental data, then the adsorption process is controlled by intra-particle diffusion. However, if the graph displays multi-linear plots, then two or more steps are involved in the adsorption process.

Table 6
Parameters of kinetic model for adsorption of Pb, Cu and Ni onto the hybrid

(T = 25°C, Ci_{metal} = 20 mg/l, pH = 8, w_{hybrid} = 0.1)							
Model	Pseudo-first-order			Pseudo-second-order			$q_{e\,exp}$
Metal	R^2	k_1	$q_{e\,cal}$	R^2	k_2	$q_{e\,cal}$	
Pb	0.22	0.01	2.79	1	∞	9.90	9.9
Cu	0.204	0.005	0.523	0.994	0.018	8.850	8.015
Ni	0.513	0.017	0.716	0.981	0.226	0.737	0.885
Model	Intra-particle diffusion			Richie			$q_{e\,exp}$
Metal	R^2	k_{id}	c	R^2	k_R	$q_{e\,cal}$	
Pb	0.63	0.12	8.57	0.35	–4.08R	9.80	9.9
Cu	0.832	0.499	2.85	0.709	0.151	8.696	8.015
Ni	0.6	0.167	–0.971	0.401	0.158	0.745	0.885

k_1(min^{-1}), q_e, q_t(mg/g), k_2(g.mg^{-1}.min^{-1}), k_{id}(mg.g^{-1}.min$^{-0.5}$), C(mg/g), k_R (1/min).

Fig. 12c shows that for all three metals, the line does not pass from the origin of the coordinates, so the surface penetration cannot be the reason for transfer of metal ions from the solution to the hybrid surface. Each of the graphs is multilinear, especially for copper, which indicates several steps occur in the adsorption process.

5.10. Isotherm adsorption models for experimental data

Investigations and studies on adsorption of isotherm have led to development of new models. In this study, four isotherm adsorption models Langmuir, Freundlich, Dubinin-Radushkevich and Temkin, have been used in order to interpret adsorption data of lead, copper, and nickel metals. These four models of isotherm adsorption are described below:

5.10.1. Langmuir

In the Langmuir model, it is assumed that 1) a layer of adsorbent material exist, 2) the surface of adsorbent is uniform, 3) there is not interaction between absorbed ions [51,52].

The Langmuir model is given as in Eq. (5):

$$\frac{1}{q_e}=\left(\frac{1}{K_L q_m}\right)\frac{1}{C_e}+\frac{1}{q_m} \tag{5}$$

where q_e, q_m, C_e, and K_L are the adsorption capacity at equilibrium (mg/g), maximum monolayer adsorption capacity (mg/g), the equilibrium concentration and Langmuir isotherm constant (L/mg), respectively.

5.10.2. Freundlich

In this model it is assumed that the adsorption process occurs at the heterogeneous surface [53], where is given as in Eq. (6).

$$Inq_e = Ink_F + \frac{1}{n} InC_e \tag{6}$$

where K_F(l/mg), $1/n$, q_e(mg/g) and C_e(mg/l) are measured the adsorption capacity, adsorption intensity, adsorption capacity and concentration at equilibrium, respectively.

5.10.3. Dubinin-Radushkevich

The Dubinin-Radushkevich (D–R) model is used for adsorption on both homogeneous and heterogeneous surfaces as well as the calculation of adsorption energy [54–56]. The (D–R) model is given as in Eqs. (7)–(9):

$$Lnq_e = Lnq_m - \beta\varepsilon^2 \tag{7}$$

$$\varepsilon = RTLn\left(1+\frac{1}{C_e}\right) \tag{8}$$

$$E_a = \frac{1}{\sqrt{2\beta}} \tag{9}$$

In the above equations, q_e(mg/g), q_m(mg/g) and β (mol²/kJ²) are three constants, which are related to adsorption capacity at equilibrium, adsorption capacity and mean free energy of adsorption, respectively. ε is a Dubinin–Radushkevich isotherm constant. C_e (mg/l), R (8.314 J/mol K), T(K) and E_a (kJ/mol) are equilibrium concentration, the gas constant, absolute temperature and the mean energy of adsorption, respectively.

5.10.4. Temkin

In the Temkin model it is assumed that with increase of the adsorbent surface coverage the adsorption heat of all molecules in the adsorbed layer is enhanced [57].

This model is described by Eq. (10):

$$q_e = \frac{RT}{b_T} LnK_T + \frac{RT}{b_T} LnC_e \tag{10}$$

where K_T is Temkin isotherm equilibrium binding constant (L/g), b_T is Temkin isotherm constant(mol/j), R is the universal gas constant (8.314 J/mol·K), T is the temperature (298K) and $B\left(\frac{RT}{b_T}\right)$ is constant related to heat of adsorption (J/mol). Table 7 lists values of the parameters of the isotherm adsorption models for the lead, copper and nickel metals.

According to Table 7, the correlation coefficient for lead in the Freundlich, Langmuir, Temkin, and Dubinin-Radushkevich models are 0.923, 0.988, 0.951, 0.953, respectively, while for copper 0.985, 0.945, 0.969, 0.926, respectively. For nickel the correlation coefficients are 0.999, 0.984, 0.983, 0.963, respectively. Comparison of the correlation coefficients for these metals clearly suggest that the using Langmuir model for lead, the Freundlich model for copper and nickel give more consistent results with the experimental data. The high values of the correlation coefficient denote that the isotherm model is very suitable for describing the adsorption of metal ions on the hybrid (see Fig. 13).

6. Discussion

Carboxylic and hydroxyl groups in nanomaterial are factors affecting the adsorption of chemical pollutants. In this study, we have shown that the presence of carboxylic and hydroxyl groups in the hybrid causes more adsorption of heavy metals. Physical and chemical properties of aqueous environments, such as pH and ionic strength, have a great influence on the adsorption of pollutants by hybrids. The effects of CNT/C60 hybrid on the absorption of heavy metals, such as copper, nickel, and lead, from water with different concentrations of adsorbent, initial concentration of metals, under pH 2 and 8 conditions have been investigated for different contact times. The capacity of metal ion absorption by the hybrid strongly depends on the total acidity of medium which is a measure of amounts of the functional groups in the medium.

Table 7
Parameters of isotherm adsorption models for the lead, copper and nickel metals

Model	Freundlich				Langmuir			TEST
Metal	*1/n*	*n*	k_f	R^2	$q_{m\,cal}$	k_1	R^2	$q_{m\,exp}$
Pb	0.275	3.636	11.870	0.923	16.67	6.7	0.988	18.80
Cu	0.238	4.202	15.180	0.985	15.15	66	0.945	20.40
Ni	0.427	2.342	24.928	0.99	22.73	11	0.984	25.20
Model	Temkin			Dubinin-Radushkevich (D–R)				TEST
Metal	K_T	b_T	R^2	β	$q_{m\,cal}$	E_a	R^2	$q_{m\,exp}$
Pb	109.17	0.895	0.951	0.023	15.8	4.7	0.953	18.80
Cu	567.85	0.989	0.969	0.009	16.5	7.5	0.926	20.40
Ni	72.58	0.457	0.983	0.02	22.6	5.0	0.963	25.20

k_f, k_1, K_T(L/g), q_m(mg/g), b_T (kJ/mol), β(mol²/kJ²), E_a(kJ/mol).

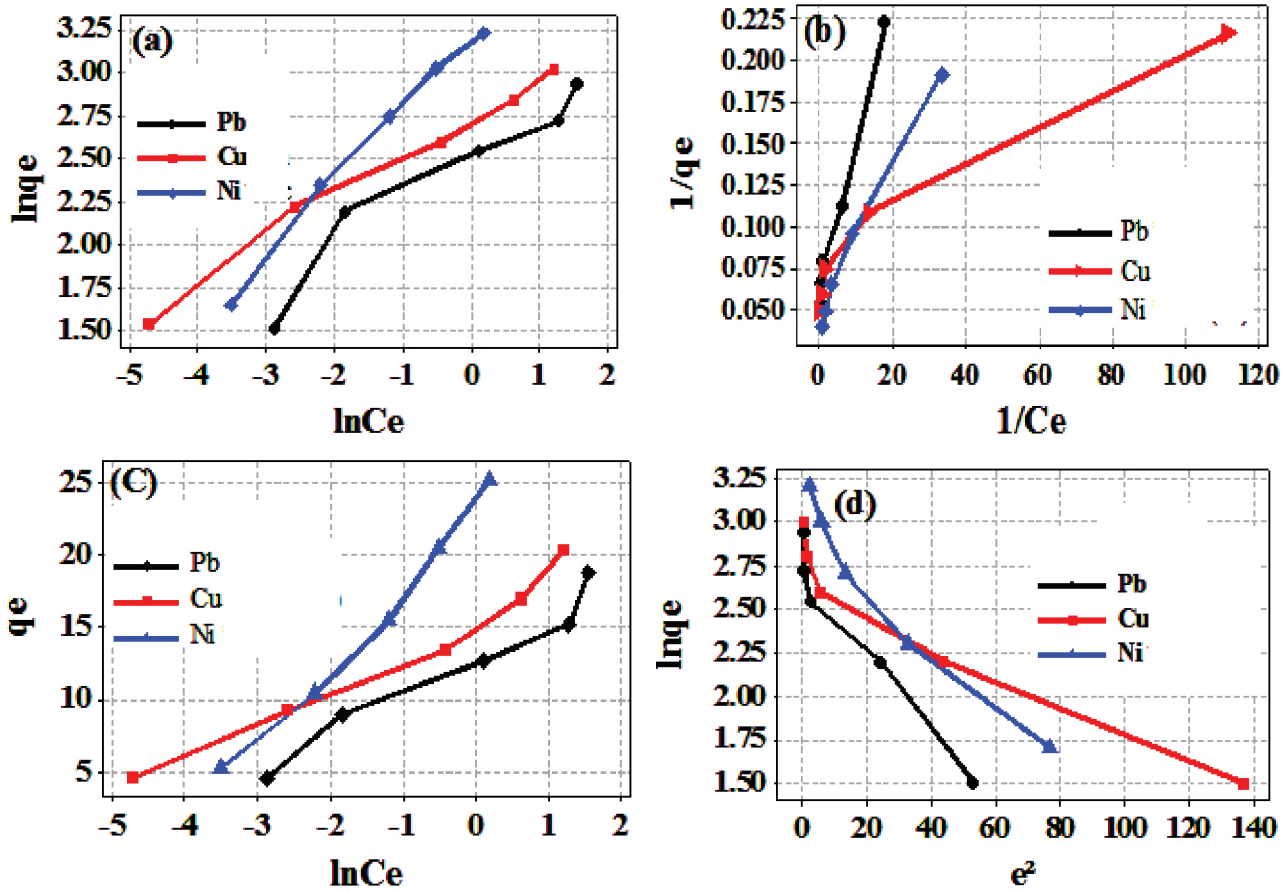

Fig. 13. Isotherm models (a) Freundlich, (b) Langmuir, (c) Temkin, (d) Dubinin- Radushkevich, for lead, copper and nickel metals (T = 25°C, pH = 8 , whybrid = 0.06 g, t = 30 min).

By examining the absorption processes in the two 2 and 8 pH conditions, it becomes clear that an effective adsorption could occur at a pH value between these two pHs. In the alkali environment containing lead and copper nitrate, in the absence of adsorbent, the metals precipitate in the form of lead and copper carbonate and the concentration of lead, copper and nickel in the solution reaches from 20 to 3.93, 17, 23.6 ppm respectively. During 30 min and at the presence of adsorbent, the concentration of lead, copper and nickel in the solution reaches from 3.93, 17, 23.6 to 0.25, 5.4, 18.07 ppm, respectively.

In every alkaline environment, some alkali compound is used to neutralize acidic substances. As a result, the carboxyl groups and negative charge are reduced which this results is reduction of metal adsorption on the hybrid surface.

The results show that the removal efficiency decreases in high acidic and increases in low alkaline environments. In the high-acidic environments the removal efficiency decreases due to the more solubility of the reaction compounds, production of high numbers of H^+, saturation of the hybrid surface with H^+ ions and strong repulsion of metal ions on sites of the adsorption.

As a result, the low numbers of metal ions are absorbed on the hybrid surface and thus concentration of the metals in the solution are almost remained constant. In the acidic environment, which is more sensitive to the removal of metals, the optimal adsorbent dose is determined to be 0.06 g. In the high acidic environment, the contact surface increases with increasing the amount of adsorbent, but the strong repulsion also increases on the hybrid surface. As a result, the percentage removal of metals is greatly reduced.

It seems pH of 2 has no advantage in the adsorption process. But in this pH, the removal of heavy metals from the hybrid surface, the recovery and regeneration of hybrids and other nanomaterials can be studied and investigated. Also, concentration of impurities on the hybrid surface reduced or even completely eliminated from the surface. Particularly, in this study, amount of the nickel metal on the hybrid surface was reduced by placing hybrid in a strong acidic solution.

The kinetic models to describe these phenomena are pseudo-first-order, pseudo-second-order, Intra-particle diffusion and Richei. The initial concentration of the metals is 20 mg/l, w –0.1 g and pH = 8.

The values of $q_{e\ cal}$ and $q_{e\ exp}$ are very close when the pseudo-second-order model is used especially for lead. The comparisons of models show that this model is more compatible with equilibrium data, thus it could better explain the adsorption of metals onto hybrid surface. The experimental values of $q_{e\,exp}$ and The calculated values of $q_{e\,cal}$ for Pb, Cu, and Ni are 9.9, 8.015, 0.885 mg/g, and 9.9, 8.850, 0.737 mg/g, respectively. The highest value of correlation coefficient is obtained in the pseudo-second-order model the R^2 for adsorption of Pb, Cu and Ni are 1, 0.994 and 0.981, respectively.

The effect of this hybrid is investigated on the adsorption of heavy metals at the initial concentration of 10–50 mg/l, pH = 8, w = 0.06 g of adsorbent and the contact time at 30 min. The results show that the optimal amount of initial concentrations is 20 mg/l and carbonate precipitates are formed for lead, copper and nickel at this pH.

The isotherm models used are Langmuir, Freundlich, Temkin and Dubinin-Radushkevich models, with initial concentration of the metal from 10 to 50 mg/l.

Langmuir adsorption model: the amount of k_1 for lead, copper and nickel is 6.7, 66, and 11, respectively, indicating that the adsorption of copper is greater than lead and nickel. In fact, large k_1, represents a great adsorption. The calculated maximum adsorption capacity, ($q_{m,cal}$) are for lead, copper, and nickel 16.67, 15.15, and 22.73, respectively. All these calculated q_m are smaller than the reported experimental data. The amount of maximum adsorption capacity (q_m) calculated may be smaller or larger than adsorption capacity of experimental data. This might be due to the large abundance of adsorbent sites and the large number of ions absorbed on the adsorbent surface as well as the high intensity of ion binding to the surface. In Table 8 the monolayer adsorption capacities for various adsorbents of the previous studies are compared to this hybrid.

Table 8
Comparison of maximum monolayer adsorption capacities of various adsorbents

Adsorbent	q_m ($mg{\cdot}g^{-1}$)	pH	Absorbed metal	Reference
Rosa Canina-L leaves ash nFe-A	588.24	6	Pb(II)	[58]
	833.33	6	Pb(II)	
SDS-AZS	18.38	6	Pb(II)	[59]
Ti(IV)	63.29	6	Pb(II)	[60]
Ti(IV)	21.32	6	Hg(II)	[61]
FSAC	80.65	4	Pb(II)	[62]
MWCNTs/ThO_2	More of 20	5.5	Pb(II)	[63]
PSTM (Polyaniline Sn(IV) (tungstomolybdate nano composite)	44.64 (20°C)	6	Pb(II)	[64]
LELP (Lycopersicum esculentum) (tomato) leaf powder)	47.61 (303 k)	5.5	Ni(II)	[65]
Nanotube-C60 hybrid	18.8	8	Pb(II)	This study
	20.4		Cu(II)	
	25.2		Ni(II)	
	1.2	2	Pb(II)	
	1.23		Cu(II)	
	0.92		Ni(II)	

Freundlich adsorption model: in this model the values of K_F (adsorption intensity) for lead, copper and nickel are 11.87, 15.18 and 24.928 l/g, respectively. This clearly indicates that adsorption capacity of nickel metal is greater than lead and copper. *1/n* denote heterogeneity of a medium, the smaller *1/n* is, the greater heterogeneity is and vice versa. Therefore, whenever the value is close to zero (very large *n* value), a higher homogeneity is expected. According to the amounts of *1/n* (adsorption intensity), the heterogeneities in lead, copper, and nickel are 0.238, 0.275 and 0.427, respectively. When the value of *1/n* is smaller than one, normal adsorption is expected. Also, the value of *1/n* closer to unity, the adsorption is more similar to the linear isotherm (more homogeneity). If value of *n* falls between one and ten, an optimal adsorption process has occurred. Table.4 shows that lead, copper and nickel adsorption are desirable. The values of *n* calculated for lead, copper and nickel are 3.636, 4.202 and 2.342, respectively.

*Tamkin adsorptionmodel:*the amounts of b_T for lead, copper and nickel ions are 0.895, 0.989, and 0.457 kJ/mol, respectively. These values indicate that the adsorption of lead ions is much easier than copper and nickel ions.The sorption process is exothermic because the heat produce during process is positive.

Dubinin-Radushkevich adsorption model: the amounts of β for lead, copper and nickel are 0.023, 0.009, and 0.02 (mol/kJ),[2] respectively. The average adsorption energy (E_a) for lead, copper and nickel are 4.7, 7.5 and 5 kJ/mol, respectively. These E_a values indicate that adsorption is a physical. Previous studies reported E_a = 1–8 and 8–16 kJ/mol, which are for physical and chemical adsorptions, respectively [66].

By comparing the experimental data with the results of models, the best model that describes the adsorption process for lead is Langmuir with correlation coefficient 0.988, for the copper and nickel is the Freundlich model with correlation coefficients 0.985 and 0.990, respectively.

7. Conclusion

In this paper, functionalized CNT/C60 hybrids was used as adsorbent to remove the heavy metals, such as lead, copper, and nickel, from aqueous environment. The preliminary studies indicated that the heavy metals are strongly adsorbed on the hybrid surface. Tests have been carried out to determine optimal adsorbent dose and contact time. The conditions with high acidity (pH 2) and alkaline (pH 8) are applied for adsorption process. Initial findings showed this hybrid was quite suitable for adsorption heavy metals. In the acidic environment, the recovery and regeneration of hybrid and other nanomaterial are possible after adsorption process. Particularly, in this study to reduce the amount of the nickel metal in the hybrid, the hybrid was placed in the strong acidic environment. The highest value of correlation coefficient is obtained in the pseudo-second-order model with R^2 for adsorption of Pb, Cu and Ni are 1, 0.994 and 0.981, respectively. The best model that can describe adsorption process for lead is Langmuir with correlation coefficient 0.9887. For the copper and nickel the best model is the Freundlich with correlation coefficients 0.985 and 0.990, respectively.

Acknowledgments

Thanks to Dr. Ahadian and lab staffs from the institute for Nanoscience & Nanotechnology (INST) Sharif University of Technology who kindly cooperate with me to carry out this research.

Symbols

C_e — Equilibrium concentration of solution, mg/L
C_i — Initial concentration of solution, mg/L
q_e — Amount of metal adsorbed per unit mass of adsorbent at equilibrium, mg/g
q_m — Langmuir constant, mg/g
q_t — Amount of metal adsorbed per unit mass of adsorbent at time t, mg/g
K_f — Freundlich constant, L/mg
K_L — Langmuir constant, L/mg
ε — Dubinin–Radushkevich isotherm constant, kJ/mol
k_T — Temkin isotherm equilibrium binding constant, L/g
k_1 — Rate constant of the pseudo-first-order adsorption process, min^{-1}
k_2 — Rate constant of pseudo-second-order adsorption, g mg^{-1} min^{-1}
K_{id} — The intra-particle diffusion constant, mg/g $min^{0.5}$
K_R — The Richie constant, 1/min
N — Freundlich constant, L/g
R — Gas constant, 8.314 J/mol/K
T — Temperature, K
B — The mean free energy of adsorption, mol^2/kJ^2
t — Time, min
b_T — The adsorption constant, J/mol K
R — Universal gas constant, 8.314 J/mol K
T — Absolute temperature value, K
B — A constant related to the heat of sorption, J/mol

References

[1] G. Busca, Technologies for the removal of phenol from fluid streams, a short review of recent developments, J. Hazard. Mater., 160 (2008) 265–288.
[2] D. Pokhrel, T. Viraraghavan, Treatment of pulp and paper mill wastewater, a review, Sci. Total Environ., 333 (2004) 37–58.
[3] A. Haritash, C. Kaushik, Biodegradation aspects of polycyclic aromatic hydrocarbons (PAHs), a review, J. Hazard. Mater., 169 (2009) 1–15.
[4] S.A. Snyder., S. Adham., A.M. Redding., F.S. Cannonc., J. DeCarolis, J. Oppenheimer, E.C. Wert, Y. Yoon, Role of membranes and activated carbon in the removal of endocrine disruptors and pharmaceuticals, Desalination, 202 (2007) 156–181.
[5] N. Bolong, A.F. Ismail, M.R. Salim, T. Matsuura, The effects of emerging contaminants in wastewater and options for their removal, A review, Desalination, 239 (2009) 229–246.
[6] W.W. Ngah, M. Hanafiah, Removal of heavy metal ions from wastewater by chemically modified plant wastes as adsorbents, a review, Biores. Tech., 99 (2008) 3935–3948.
[7] S.E. Bailey, T.J. Olin, R.M. Bricka, D.D. Adrian: A review of potentially low-cost sorbenls for heavy metals, Water Res., 33 (1999) 2469–2479.
[8] N. NHMRC, Australian drinking water guidelines paper 6 national water quality management strategy, National Health and Medical Research Council, National Resource Management Ministerial Council, Commonwealth of Australia, Canberra, 2004.
[9] F. Su, C. Lu, Adsorption kinetics, thermodynamics, and desorption of natural dissolved organic matter by multiwall carbon nanotubes, Environ. Sci. Health A., 42 (2007) 1543–1552.
[10] W. Cheng, S.A. Dastgheib, T. Karanfil, Adsorption of dissolved natural organic matter by modified activated carbons, Water Res., 39 (2005) 2281–2290.
[11] R.C. Hoehn, BW. Long, Toxic cyanobacteria (blue green algae): an emerging concern. In: Envirologix, editor. Natural Water Toxins. 2008. Envirologix, Portland, 1999.
[12] J.O. Duruibe, M.O.C. Ogwuegbu, J.N. Egwurugwu, Heavy metal pollution and human biotoxic effects, Phys. Sci., 2 (2007) 112–118.
[13] V.K.K. Upadhyayula, S.G. Deng, M.C. Mitchell, G.B. Smith, Application of carbon nanotube technology for removal of contaminants in drinking water, Sci. Total Environ., 408 (2009) 1–13.
[14] J.G. Yu, X.H. Zhao, L.Y. Yu, F.P. Jiao, J.H. Jiang, X.Q. Chen, Removal, recovery and enrichment of metals from aqueous solutions using carbon nanotubes, Radioanal. Nucl. Chem., 299 (2014) 1155–1163.
[15] N. Mubarak, J. Sahu, E. Abdullah, N. Jayakumar, Removal of heavy metals from wastewater using carbon nanotubes, Sep. Purif. Rev., 43 (2014) 311–338.
[16] X. Ren, C. Chen, M. Nagatsu, X. Wang, Carbon nanotubes as adsorbents in environmental pollution management, a review, Chem. Eng. J., 170 (2011) 395–410.
[17] D.Y. Lyon, D.A. Brown and P.J.J. Alvarez., Implications and potential applications of actericidal fullerene water suspen-

sions: effect of nC60 concentration, exposure conditions and shelf life, Water Sci. Tech., 57 (2008) 1533–1538.
[18] H.W. Kroto, J.R. Heath, S.C. O'Brien, R.F. Curl, R.E. Smalley, C60: Buckminster-fullerene, Nature, 318 (1985) 162–163.
[19] S. Iijima, Helical microtubules of graphitic carbon, Nature, 354 (1991) 56–58.
[20] A. Hirsch, C. Bellavia-Lund, Fullerenes and Related Structures, (A. Hirsch Ed.). Berlin: Springer, 1999.
[21] L.Y. Chiang, J.W. Swirczewski, C.S. Hsu, S.K. Chowdhury, S. Cameron, Multi-hydroxy additions onto C60 fullerene molecules, Chem. Comm., 24 (1992) 1791–1793.
[22] L.Y. Chiang, R.B. Upasani, J.W. Swirezewski, S. Soled, Evidence of hemiketals incorporated in the structure of fullerols derived from aqueous acid chemistry, J. Am. Chem. Soc., 115 (1993) 5453–5457.
[23] J. Li, A. Takeuchi, M. Ozawa, XH. Li, K. Saigo, K. Kitazawa, C60 fullerol formation catalysed by quaternary ammonium hydroxides, Chem. Comm., 23 (1993) 1784–1785.
[24] S. Wang, P. He, J. Yhang, H. Jiang, S. Zhu, Novel and efficient synthesis of water-soluble 60 fullerenol by solvent-free reaction, Syn. Comm., 35 (2005) 1803–1808.
[25] G. Zhang, Y. Liu, D. Liang, L. Gan, Y. Li, Facile synthesis of isomerically pure fullerenols and formation of spherical aggregates from C60(OH)8, Angewandte Chemie Int. Ed., 49 (2010) 5293–5295.
[26] K. Kokubo, K. Matsubayashi, H. Tategaki, H. Takada, T. Oshima, Facile synthesis of highly water-soluble fullerenes more than half-covered by hydroxyl groups, ACS Nano, 2 (2008) 327–333.
[27] H. Paloniemi, T. Aaritalo, T. Laiho, H. Liuke, N. Kocharova, K. Haapakka, F. Terzi, R. Seeber, J. Lukkari, Water-soluble full-length single-wall carbon nanotube polyelectrolytes: preparation and characterization, J. Phys. Chem. B, 109 (2005) 8634–8642.
[28] N. Hu, G. Dang, H. Zhou, J. Jing, C. Chen, Efficient direct water dispersion of multi-walled carbon nanotubes by functionalization with lysine, Mater. Lett., 61 (2007) 5285–5287.
[29] X.F. Zhang, T.V. Sreekumar, T. Liu, S. Kumar, Properties and structure of nitric acid oxidized single wall carbon nanotube films, J. Phys. Chem. B, 108 (2004) 16435–16440.
[30] A.G. Rinzler, J. Liu, H. Dai, P. Nikolaev, C.B. Huffman, F.J. Rodriguez-Macias, P.J. Boul, A.H. Lu, D. Heymann, D.T. Colbert, R.S. Lee, J.E. Fischer, A.M. Rao, P.C. Eklund, R.E. Smalley, Large-scale purification of single-wall carbon nanotubes: process, product, and characterization, App. Phys. Mat. Sci. Proc., 67 (1998) 29–37.
[31] Q. Liao, J. Sun, L. Gao, Adsorption of chlorophenols by multiwalled carbon nanotubes treated with HNO_3 and NH_3, Carbon., 46 (2008) 553–555.
[32] S. Zhang, T. Shado, S.S. Bekaroglu, T. Karanfil, The impacts of aggregation and surface chemistry of carbon nanotubes on the adsorption of synthetic organic compound, Environ. Sci. Technol., 43 (2009) 5719–5725.
[33] N. Martin, J.F. Nierengarten, Supramolecular chemistry of fullerenes and carbon nanotubes, G. Francesco, A. Herranz, M. Nazario, Carbon Nanostructures: Covalent and Macromolecular Chemistry, Wiley–VCH, Germany, 2012.
[34] B.W. Smith, M. Monyhious and D.D. Luzzi, Encapsulated C60 in carbon nanotubes, Nature., 396 (1998) 323–324.
[35] A.B. Bourlinos, V. Georgakilas, A. Bakandritsos, A. Kouloumpis, D. Gournis, R. Zbori, Aqueous-dispersible fullerol-carbon nanotube hybrids, Mater. Lett., 82 (2012) 48–50.
[36] VK. padhyayula, S. Deng, MC. Mitchell, GB. Smith, Application of carbon nanotube echnology for removal of ontaminants in drinking water, a review, Sci. Total Environ., 408 (2009) 1–13.
[37] M.E. Milanesio, M.B. Spesia, M.P. Cormick, E.N. Durantini, Mechanistic studies on the photodynamic effect induced by a dicationic fullerene C60 derivative on Escherichia coli and Candida albicanscells, Photodiagn. Photodyn. Therapy, 10 (2013) 320–327.
[38] X. Tao, Y. Yu, J.D. Fortner, Y. He, Y. Chen, J.B. Hughes, Effects of aqueous stable fullerene nanocrystal (nC60) on Scenedesmusobliquus, Chemosphere, 122 (2014) 162–167.
[39] B. Fugetsu, S. Satoh, T. Shiba, T. Mizutani, Y.B. Lin, N. Terui, Y. Nodasaka, K. Sasa., K. Shimizu, T. Akasaka, Caged multiwall carbon nanotubes as the adsorbents for affinity-based elimination of ionic dyes, Env. Sci. Technol., 38 (2004) 6890–6896.
[40] X.J. Peng, Y.H. Li, Z.K. Luan, Z.C. Di, H.Y. Wang, B.H. Tian, Z.P. Jia, Adsorption of 1,2-dichlorobenzene from water to carbon nanotubes, Chem. Phys., 376 (2003) 154–158.
[41] M. Calvaresiand, F. Zerbetto, The devil and holy water: protein and carbon nanotube hybrids, Acc. Chem. Res., 46 (2013) 2454–2463.
[42] Y.H. Li, J. Ding, Z.K. Luan, Z.C. Di, Y.F. Zhu, C.L. Xu, D.H. Wu, B.Q. Wei, Competitive adsorption of Pb2+, Cu2+ and Cd2+ ions from aqueous solutions by multiwall carbon nanotubes, Carbon, 41 (2003) 2787–2792.
[43] Q. Liu, Q. Cui, X. J. Li, L. Jin, The applications of buckminsterfullerene C60 and derivatives in orthopaedic research, Connect Tissue Res., 55(2014) 71–79.
[44] D.Y. Lyon, D.A. Brown, P.J.J. Alvarez., Implications and potential applications of actericidal fullerene water suspensions: effect of nC60 concentration, exposure conditions and shelf life, Water Sci. Tech., 57 (2007) 1533–1538 en.wikipedia.org/wiki/Solubility_table, 2018.
[45] D.D. Amarendra, P.D. Shashi, G. Krishna, S. Mika., Strengthening adsorptive amelioration: Isotherm modeling in liquid phase surface complexation of Pb(II) and Cd(II) ions, Desalination, 267 (2010) 25–33.
[46] S. Lagergren, About the theory of so called adsorption of solute substances, Ksver Veterskapsakad Handl., 24 (1898) 1–6.
[47] Y.S. Ho, G. McKay, The sorption of lead (II) ions on peat, Water Res., 33 (1999) 578–584.
[48] T.W. Weber, R.K. Chatravorti, Pore and solid diffusion models for fixed bed adsorbers, Am. Inst. Chem. Eng., 20 (1974) 228–238.
[49] AG. Ritchie, Alternative to elovich equation for kinetics of adsorption of gases on solids. Chem. Soc., Faraday Trans., 73 (1977) 1650–1653.
[50] Y.S. Ho, G. McKay, Competitive sorption of copper and nickel ions from aqueous solution using peat, Adsorption, 5 (1999a) 409–417.
[51] R. Prabakaran, S. Arivoli, Biosorption of Ferrous Ion from Aqueous Solutions by using Activated carbon prepared from Thespesia Populnea Bark, Arch. Appl. Sci. Res., 3 (2011) 218–232.
[52] H.M.F. Freundlich, Over the adsorption in solution, Phys. Chem., 57(1906) 385–471.
[53] M.M. Dubinin, L.V. Radushkevich, The equation of the characteristic curve of the activated charcoal, Proc. Acad. Sci. USSR Phys. Chem. Sect., 55 (1947) 331–337.
[54] W. Rondon, D. Freire, Z. de Benzo, A.B. Sifontes, Y. González, M. Valero, J.L. Brito, Application of 3A zeolite prepared from venezuelan kaolin for removal of Pb(II) from wastewater and its determination by flame atomic absorption spectrometry, Am. J. Anal. Chem., 4 (2013) 584–593.
[55] H. Chen, J. Zhao, G. Dai, J. Wu, H. Yan., Desorption characteristics of Pb(II) from aqueous solution onto a natural biosorbent, Fallen Cinnamomum camphora Lyeaves, Desalination, 262 (2010) 174–182.
[56] S.N. Dash, R. Murthy, Preparation of carbonaceous heavy metal adsorbent from Shorea robusta leaf litter using phosphoric acid impregnation, Env. Sci., 1 (2010) 296–313.
[57] M. Ghasemi, M. Naushad b, N. Ghasemi, Y. Khosravi-fard, Adsorption of Pb(II) from aqueous solution using new adsorbents prepared from agricultural waste: Adsorption isotherm and kinetic studies, Ind. Eng. Chem., 20 (2014) 2193–2199.
[58] M. Naushad, Surfactant assisted nano-composite cation exchanger: Development, characterization and applications for the removal of toxic Pb^{2+} from aqueous medium, Chem. Eng., 235 (2014) 100–108.

[59] M. Naushad, Z.A. ALOthman, M. Rabiul Awual, M.M. Alam, G.E. Eldesoky, Adsorption kinetics, isotherms, and thermodynamic studies for the adsorption of Pb^{2+} and Hg^{2+} metal ions from aqueous medium using Ti(IV) iodovanadate cation exchanger, Ionics, 21 (2015) 2237–2245.
[60] M. Ghasemi, M. Naushad, N. Ghasemi, Y. Khosravi-fard, A novel agricultural waste based adsorbent for the removal of Pb(II) from aqueous solution: Kinetics equilibrium and thermodynamic study, Ind. Eng. Chem., 20 (2014) 454–461.
[61] A. Mittal, M. Naushadb, G. Sharmac, Z.A. ALothmanb, S.M. Wabaidur, M. Alam, Fabrication of MWCNTs/ThO2 nanocomposite and its adsorption behavior for the removal of Pb(II) metal from aqueous medium, Desal. Water Treat., 57 (2016) 21863–21869.
[62] R. Bushra, M. Naushad, R. Adnan, M.N.M. brahima, M. Rafatullah, Polyaniline supported nanocomposite cation exchanger: Synthesis, characterization and applications for the efficient removal of Pb^{2+} ion from aqueous medium, Ind. Eng. Chem., 21 (2015) 1112–1118.
[63] Y. Guthaa, V.S. Munagapati, M. Naushadc and K. Abbur., Removal of Ni(II) from aqueous solution by Lycopersicum esculentum (Tomato) leaf powder as a low-cost biosorbent, Desal. Water Treat., 54 (2015) 200–208.
[64] A.N. Siyal, S.Q. Memon, M.I. Khaskheli, Optimization and equilibrium studies of Pb(II)removal by Grewia Asiatica seed: a factorial design approach, Polish J. Chem. Technol., 14 (2012) 71–77.